DEUTSCHES ELEKTRONEN-SYNCHROTRON DESY

DESY 87-092
August 1987

MONTE CARLO SIMULATION OF A LATTICE FIELD THEORY AS CORRELATED PERCOLATION

by

U. Wolff

Institut f. Theoretische Physik, Universität Kiel

ISSN 0418-9833

NOTKESTRASSE 85 · 2 HAMBURG 52

To be sure that your preprints are promptly included in the
HIGH ENERGY PHYSICS INDEX ,
send them to the following address (if possible by air mail) :

DESY
Bibliothek
Notkestrasse 85
2 Hamburg 52
Germany

DESY 87-092
August 1987

ISSN 0418-9833

MONTE CARLO SIMULATION OF A LATTICE FIELD THEORY AS CORRELATED PERCOLATION

Ulli Wolff

Institut für Theoretische Physik, Universität Kiel,
D-2300 Kiel, West Germany

Abstract

The recently proposed formulation of lattice field theory as a pecolation process is tested numerically in the O(3) σ-model. Its spins decompose into fluctuating clusters similar to Fisher droplets. We use the explicitly available cluster structure to perform collective moves reducing autocorrelation times and to define improved estimators for physical observables. On a 56^2 lattice gains in computer time efficiency up to a factor 5 are realized.

1. Introduction

Monte Carlo simulation on computers has become a standard tool to extract information from models in statistical mechanics and field theory. Most physically interesting features of these models are related to their long range collective behavior which can be accurately calculated analytically in exceptional cases only. Since the simulation is always (much too) finite we have to introduce cutoffs whereever nature is truely or effectively infinite. In field theory the introduction of a finite volume together with a finite resolution in the form of a nonzero lattice spacing are prerequisites for a numerical simulation. Since in our present understanding these scales are artificial rather than constants of nature, observable results have to be insensitive to their values once the cutoffs are remote from physical scales. From the statistical mechanics point of view one is thus required to work with large correlation lengths which are still small compared to the linear system dimension. This clearly calls for large lattices. If one is enabled to increase the lattice size- for instance by the advent of a new computer generation- one may either expand the simulated volume or shrink the lattice spacing.

Great progress has been made in understanding the approach to the infinite volume limit[1]. The asymptotic dependence on the volume of an underlying torus can be extrapolated with good confidence and even be used to obtain information about scattering. For the lifting of the ultraviolet cutoff universality and the renormalization group[2] provide an understanding and a parametrization. This, however, seems to be a more problematical limit at present. Even in asypmtotically free theories, where the asymptotic dependence on the lattice spacing is known and no critical exponents have to be fitted, it is still to some degree controversial when and where scaling sets in. Consequently one may want

to use larger lattices mainly to reduce the lattice spacing, i.e. get closer to criticality. The additional problem of critical slowing down[3] has then to be faced. Clearly the computing time for one pass through the lattice is proportional to the number of degrees of freedom. In the critical region estimates for observables derived from successive configurations produced with standard local algorithms become more and more statistically dependent. The computer time needed to measure a quantity to a given accuracy then grows with a higher power of the lattice size. Physically the reason is that the long wavelength fluctuations are inefficiently sampled by the local updates. Improved behavior in this respect can only[4] be hoped for, if we design algorithms performing collective moves of many variables. Previous attempts aiming in this direction are Fourier acceleration[5,6] and multigrid methods[7].

Recently Swendsen and Wang[8](SW) have put forward an amazingly efficient algorithm for models involving Potts spins. It is based on the numerical exploitation of an alternative but equivalent representation of the model by Fortuin and Kasteleyn[9](FK) which is closely related to percolation theory. In this article we explore a generalization of this method to arbitrary and in particular to continuous fields.

The paper is organized as follows: In sect. 2 we review the FK-representation in a form also useful for non-Potts models. In sect. 3 a microcanonical variant of the SW-algorithm is constructed and briefly tested in the Ising model. This is followed in sect. 4 by the report of extensive numerical studies for the asymptotically free O(3) σ-model in two dimensions. Finally sect. 5 contains conclusions and open questions.

2. Dynamical Dilution

The method of introducing additional two valued bond variables as dynamical fields (annealed summation) in spin models has already been briefly introduced in [10]. Here we start with a rather general lattice system with dynamical variables φ_r, where r are sites, links or even higher dimensional objects. A number of them interacts locally on bonds b (links, plaquettes, etc.). The partition function of such a system is given by

$$Z = \int \prod_r d\mu(\varphi_r)\, e^{\sum_b s_b(\varphi_r)} \,. \tag{2.1}$$

Both the integration measure $d\mu(\varphi_r)$ and the one-bond action[#1] $s_b(\varphi_r)$ determine the invariance properties, and each s_b depends only on the φ_r connected by bond b ($r \in b$). By the introduction of a dynamical field k_b with values 0 and 1 on the bonds a new and in general different model results with partition function

$$\overline{Z} = \sum_{\{k_b=0,1\}} \int \prod_r d\mu(\varphi_r)\, e^{\sum_b k_b [\varkappa + s_b(\varphi_r)]} \,. \tag{2.2}$$

A chemical potential $\varkappa$ for bonds has been included as a free parameter, and for $\varkappa \to \infty$ the bonds will freeze to $k_b=1$ bringing us back to the original model up to a trivial normalization factor. Of course we are interested in new members of the family of models (2.2) with $\varkappa < \infty$. Then, for a typical given configuration $\{k_b\}$, the model is diluted as part of the interaction bonds are absent. The variables φ_r may be grouped into a maximal number of N_c independent clusters c such that there are no active bonds($k_b=1$) between φ_r in different clusters. A consequence is that each cluster enjoys the symmetry of the whole system (global spin rotations, gauge invariance)

independently. The number and shape of clusters is a complicated function of the bond variables and fluctuates. Nevertheless, at least for standard cases like bonds on links corresponding to nearest neighbor spin models, algorithms[11] are known from percolation theory that identify clusters very efficiently. In particular the time to do so grows only linearly with the volume. Explicit knowledge of the clusters may then be used to perform large collective moves along constant action surfaces in the simulation of (2.2): each cluster is moved as a whole by a randomly chosen member of the symmetry group. Such moves interspersed between standard update sweeps on $\{k_b, \varphi_r\}$ may very well result in an improved algorithm at reasonable cost in computer time. Let us now think of s_b as an action of ferromagnetic character that is maximal for configurations like aligned spins or pure gauges. Then (2.2) shows a tendency to have active bonds between aligned variables and vice versa. Clearly the clusters will bear at least qualitative resemblance with Fisher droplets[12].

It is time now to discuss what kind of system actually has resulted from introducing the bond variables in (2.2). Although we plan to numerically simulate the joint distribution $\{k_b, \varphi_r\}$ we may also perform the k_b – summation exactly producing an effective action $\bar{s}_b(\varphi_r)$,

$$\bar{s}_b(\varphi_r) = \log\left[\left(1+e^{\varkappa+s_b(\varphi_r)}\right)/\left(1+e^{\varkappa}\right)\right]. \qquad (2.3)$$

Here the irrelevant constants in s_b, $\bar{s}_b$ have been fixed by demanding them to vanish for classical configurations of maximal Boltzmann weight denoted by $\varphi_r = 1$

$$s_b(\varphi_r=1) = 0 = \bar{s}_b(\varphi_r=1). \qquad (2.4)$$

The new action is trivially of the same geometrical structure (nearest neighbor, one-plaquette etc.) as the original one. Also, if s_b is ferromagnetic, so is $\bar{s}_b$, but the suppression of non-aligned configurations has become weaker since

$$0 < \frac{d\bar{s}_b}{ds_b} = \left(1+e^{-\varkappa-s_b}\right)^{-1} < 1. \qquad (2.5)$$

Obviously ferromagnetism has weakend as each bond is active only "part of the time" for $\varkappa<\infty$.

The simplest cases with regard to transformation (2.3) are q-state Potts models. Their bond actions are only capable of two different values $s_b(\varphi_r)\in\{0,-K\}$ for any configuration of the q-valued φ_r. Then $\bar{s}_b$ is a Potts action, too, with

$$-\bar{K} = \log\left[\left(1+e^{\varkappa-K}\right)/\left(1+e^{\varkappa}\right)\right]. \qquad (2.6)$$

Each Potts theory of fixed $\bar{K}$ is exactly equivalent to a one parameter family of dynamically diluted models. Its extremal member at $K=\infty$, $\varkappa=\log(e^{\bar{K}}-1)$ corresponds to the FK-representation used by SW. The φ_r-integration in (2.2) then degenerates to counting the number of φ_r-configurations that saturate all bonds by $s_b(\varphi_r)=0$. In the simple nearest neighbor Potts spin model all spins have to be parallel and equal to one of the q possible values thus entailing the weight factor q^{N_c}[9]. Although the terminology is somewhat different, SW[8] effectively simulate the joint distribution of $\{k_b, \varphi_r\}$ at $K=\infty$. For the critical Ising model in two dimensions they find an energy autocorrelation time τ growing as $\tau \propto L^{0.35}$, when L is the side length of a square lattice. This clearly represents quite an appreciable improvement over standard local algorithms with $\tau \propto L^{2.125}$ (see also sect. 3).

Most lattice models whose scaling limits are of interest as quantum field theories possess continuous spin or gauge field variables. Then in general $\bar{s}_b$ will have a different functional dependence on ψ_r than s_b for any $\varkappa<\infty$. One strategy that comes to mind is to try to find an s_b such that $\bar{s}_b$ coincides with some standard action for the model at hand. In practical applications we found this inefficient if at the same time all weights in (2.2) are kept positive (real $s_b, \varkappa$). If we evaluate (2.3) for fields that receive maximal suppression $\bar{s}_b=-\Delta$ (like antiparallel spins at b) we find an inequality

$$\varkappa \geq \Delta + \log\left(1-e^{-\Delta}\right). \qquad (2.7)$$

Close to the scaling limit it seems very unnatural in continuous models that the bond chemical potential is essentially determined by the energy penalty for maximally frustrated bonds. We found that when this is tried for the $\in$-model, bonds practically never break. We then decided to choose a readily implementable standard form for s_b and to work with the $\bar{s}_b$ that we are able to produce by tuning $\varkappa$ and the parameters in s_b. We assume-as far as long range physics is concerned- that this is covered under the umbrella of universality: If tuning leads to long range correlations, we expect to see universal features of the theory that are independent of details in the lattice action. At present it is not clear to us to which degree of rigor this can actually be established analytically, or if the new kind of action may even approach the continuum more smoothly.

It may be noted that on the one hand there is an infinite set of extra terms, when $\bar{s}_b$ is expanded in terms of s_b. On the other hand, since we stick to effective actions of one and the same range and geometry, they are in a way all neighbors in the space of all conceivable actions[2,13]. One could also regard the fluctuating linkage of degrees of freedom as a step in the direction

of a random lattice[14]. Among the other acceleration methods the multigrid formalism[7] is closest to the method presented here. There the clusters are chosen "by hand" in a hierarchical order while we "derive" them in a stochastic way correlated with the energy fluctuations of the fields. An advantage of the multigrid algorithms is presumably that they allow to test a more general class of collective moves which are only conditionally accepted.

3. Microcanonical Algorithm for Diluted Models

The number of active bonds mediating interactions between fields $N_b = \sum_b k_b$ is a simple observable in system (2.2). It is an extensive variable equal to a fraction p_b of all possible bonds N_b^{max} which we assume to be of the order of the number of lattice sites,

$$\langle N_b \rangle = p_b N_b^{max}. \tag{3.1}$$

For given actions s_b the bond fraction p_b will be a monotonically growing function of $\varkappa$. According to the general principles of thermodynamics fluctuations in N_b will be irrelevant in the large lattice limit. Instead of adjusting $\varkappa$ to produce a desired value for p_b we may equally well directly restrict the values N_b in the sum over configurations (microcanonical ensemble)

$$Z_m(\bar{N}_b) = \sum_{\{k_b\}} \int \prod_r d\mu(\varphi_r)\, e^{\sum_b k_b s_b(\varphi_r)} \delta_{\sum_b k_b, \bar{N}_b}, \tag{3.2}$$

from which the canonical partition function may be reconstructed

$$Z = \sum_{\bar{N}_b=0}^{N_b^{max}} e^{\varkappa \bar{N}_b}\, Z_m(\bar{N}_b). \tag{3.3}$$

Following Creutz[15] a practical method to perform a microcanonical simulation consists of adding one (or several) degrees of freedom called demon(s) to the system and evaluating

$$Z_b(\bar{\bar{N}}_b) = \sum_{k_D=0}^{\infty} Z_m(\bar{N}_b)\, \delta_{\bar{N}_b - k_D, \bar{\bar{N}}_b}. \tag{3.4}$$

The advantage of having the demon is that it relaxes the constraint by reintroducing microscopic fluctuations[#2] in N_b for finite volume and thus allows a local bond by bond updating. Moreover, it functions as a "thermometer" because k_D is distributed according to the same "temperature" as the bonds namely the chemical potential $\varkappa$

$$p(k_D) \propto e^{-\varkappa k_D} \Rightarrow \varkappa = \log(1 + 1/\langle k_b \rangle). \tag{3.5}$$

The $\varkappa$-value for an equivalent canonical simulation may thus be found by observing the bond content k_D of the demon. Obviously the relation

$$Z_b(\bar{\bar{N}}_b) = \sum_{\bar{N}_b} Z_m(\bar{N}_b)\, \Theta(\bar{N}_b - \bar{\bar{N}}_b) \tag{3.6}$$

connects the strictly microcanonical Z_m and the demon ensemble Z_D. To summarize, all three ensembles Z (2.2), Z_m (3.2), Z_D (3.4) are equivalent in the large lattice limit when fluctuations of N_b become unimportant; at a more formal level this may be verified by saddle point expansions in the inverse volume.

Originally we thought that it was simply more convenient to control p_b instead of $\varkappa$. From uncorrelated bond percolation[16] we have some experience that typical bond probabilities around 0.5 lead to nontrivial cluster structure. In practice it turned out that even for the Ising model a microcanonical version of the SW-simulation brings about considerable further improvement, as will be shown in the remainder of this section. For the O(3) σ-model we completely switched to the microcanonical control of bond occupation after a few initial experiments with the canonical form.

To specialize the general concepts developed so far to the Ising model on an L^2 lattice we replace $r \to x$, $b \to x\mu$, $\varphi_r \to \sigma_x = \pm 1$, $s_b \to \beta(\sigma_x\sigma_{x+\mu} - 1)$. The canonical and the demon partition functions read

$$Z = \sum_{\substack{\{k_{x\mu}=0,1\} \\ \{\sigma_x = \pm 1\}}} e^{\sum_{x\mu} k_{x\mu}[\varkappa + \beta(\sigma_x\sigma_{x+\mu} - 1)]} \tag{3.7}$$

and

$$Z_D = \sum_{\substack{\{k_{x\mu}=0,1\} \\ \{\sigma_x = \pm 1\}}} e^{\beta \sum_{x\mu} k_{x\mu}(\sigma_x\sigma_{x+\mu} - 1)} \, \Theta\left(\sum_{x\mu} k_{x\mu} - \bar{p}_b 2L^2\right). \tag{3.8}$$

In (3.8) the sum over demon bonds has been carried out and, comparing with (3.5), k_D has now been replaced by the excess bonds (argument of the θ-function).

To test the microcanonical algorithm by comparison with ref.[8] we ran simulations for the Ising model at the (infinite volume) critical point. For the usual formulation ($K = \infty$) it is located at $\beta_c = \frac{1}{2}\log(1+\sqrt{2})$. According to (2.6) applied to the Ising model (two state Potts model) this implies criticality for all $(\beta, \varkappa)$ fullfilling

$$\frac{1 + e^{\varkappa - 2\beta}}{1 + e^{\varkappa}} = e^{-2\beta_c} = \sqrt{2} - 1 . \tag{3.9}$$

In particular the FK-limit is included at $\beta = \infty$, $\varkappa = \log(e^{2\beta_c} - 1) = \frac{1}{2}\log 2 =: \varkappa_c$. The results of our Ising simulation are shown in table 1. On square lattices of sizes L=20, 40, 80 we ran three types of simulations: Type 1 are standard heatbath runs at β_c with all bonds in place. In type 2 runs we put $\beta = \infty$ and update the $k_{x\mu}$-variables according to (3.7) with $\varkappa = \varkappa_c$; these runs are of the same

kind as in ref.[8]. For type 3 runs we use our new microcanonical formulation (3.8) at $\beta = \infty$. From exact results as well as from our type 2 simulation we know that we have $p_b = \frac{1}{2}$ at criticality, and consequently we use this value as an input parameter in our type 3 runs ($\bar{p}_b$ in (3.8)). Incidentally $p_b = \frac{1}{2}$ is also the percolation threshold for uncorrelated link percolation[#3] on a two dimensional square lattice[17]; such a coincidence between Ising and percolation criticality ceases however to be true in three dimensions[18]. After each update sweep on $\{k_{x\mu}\}$ in type 2,3 calculations we run the Hoshen-Kopelman algorithm[11] to sort out the clusters. It produces a label for each spin that uniquely denotes the cluster that the spin belongs to. Then one of the two spin orientations is randomly assigned to the cluster as a whole. A new bond sweep follows where $\beta = \infty$ is taken into account by never activating a bond between opposite spins. We call this whole sequence of operations one sweep. The number of sweeps constituting each simulation is quoted in the tables in multiples of 1000. Note in which way the cluster structure is allowed to fluctuate: bonds within a cluster may break with probability $(1+e^{\varkappa})^{-1}$, while broken bonds between different clusters of the same spin orientation may be switched on with the complementary probability.

Beside the average number N_C of clusters (not including one-spin clusters for technical reasons) we report values and autocorrelation times for two kinds of observables in table 1. The nearest neighbor correlation E is defined as

$$E = \frac{1}{2L^2} \left\langle \sum_{x\mu} \sigma_x \sigma_{x+\mu} \right\rangle \tag{3.10}$$

and the (unsubtracted) magnetic susceptibility χ as

$$\chi = \frac{1}{L^2} \left\langle \left(\sum_x \sigma_x \right)^2 \right\rangle . \qquad (3.11)$$

We use it as a simple quantity sensitive to long distance behavior. Instead of χ we actually quote the susceptibility per volume $C=\chi/L^2$, $0 \leq C \leq 1$. For our numerical work we used improved estimators for E and C. They take into account that correlations between spins in different clusters would vanish exactly if the complete spin summations were carried out for each $\{k_{x\mu}\}$ configuration. This guarantees E and χ to be also given by

$$E = \frac{1}{2L^2} \left\langle \sum_{x\mu} \sigma_x \sigma_{x+\mu} \theta(x, x+\mu; k_{x\mu}) \right\rangle \qquad (3.12)$$

and

$$\chi = \frac{1}{L^2} \sum_c \left\langle \left(\sum_{x \in c} \sigma_x \right)^2 \right\rangle . \qquad (3.13)$$

Here $\theta(x,y;k_{x\mu})$ equals unity if x and y are in the same cluster associated with $\{k_{x\mu}\}$ and vanishes otherwise. The sum in (3.13) is over all clusters c, i.e. the susceptibility is additive in the clusters. We found these improved estimators to have the same means but smaller variances than the naive ones. This is intuitively understandable[19]: Instead of sampling one random member of a set of configurations whose contributions cancel exactly we just record a zero. One could say that in this way by symmetry we take into account more spin configurations than actually appear in the computer memory. In our measurements we found a medium size benefit from using improved estimators; a typical finding was a saving of $\sim 40\%$ sweeps to measure χ to given accuracy. For measuring masses from purely long distance correlations this could become more dramatic.

Autocorrelation times have been estimated by monitoring the connected correlation function in time (number of sweeps) of the measured quantities for about 3τ. The error estimates on τ are derived "by eye" only from the

oscillations in the ratios of successive values of the correlation function over the plateau were they are stable and not yet swamped by noise. Some multiple independent runs have been made to see consistency, too. The errors quoted for observables take into account the measured correlations up to the window described above and add the tail as extrapolated by a pure exponential with the estimated τ. The quantities A_E and A_C are products of the mean square deviation and the autocorrelation time for the respective observables. If the correlation is simply exponential in time, then $\sqrt{2A/N}$ is the error if N sweeps with correlation time $1 \ll \tau \ll N$ are made. This is the rule that it takes $\sim 2\tau$ sweeps[20] to produce an independent estimate. Our more refined errors usually deviate from the above estimate only by small margins. We propose A as a convenient measure to compare different algorithms. The ratio of A-values equals the inverse ratio of the number of sweeps necessary to achieve the same accuracy.

With all this said we see the enormous advantage of type 2,3 runs over standard type 1 simulations from table 1. Our data are compatible with the same growth rate in τ vs. L for type 2 and 3, but correlation times are cut by another factor ~ 2 and the improved observables are less noisy for case 3. Results from type 1 and 2 are always compatible within errors as they have to be, and correlation times for the latter agree well with ref.[8]. Small deviations between 2 and 3 are finite volume effects of order $1/L^2$. Due to physical rounding of the phase transition and for 3 also due to the presence of the demon, in neither case p_b equals 0.5 exactly. We rather find for instance $p_b=0.5011$ for type 2 and $p_b= .5002$ for type 3 on the 80^2 lattice. We conclude that the microcanonical algorithm works well, and on the L=80 lattice, it reduces the needed number of sweeps by another factor of ~ 16 for E and by ~ 5 for C. Returning to the standard algorithm one feels somewhat like trading a razor blade for a mallet.

4. Simulation of the O(3) Nonlinear σ-Model

All Ising model formulas in the last section carry over to O(n) σ-models if products of spins are interpreted as the appropriate O(n) invariant contractions, and if sums over spin orientations are replaced by integrations over spheres S_{n-1} at each site. Our numerical work will be concerned with n=3, the minimal n for asymptotic freedom in two dimensions. The O(3) σ-model is a standard testing ground for methods to be applied to nonabelian gauge theory. There exists a large amount of reliable reference data in the literature[21].

For the dynamically diluted σ-model the (canonoical) partition function may be written in the suggestive form

$$Z = \sum_{\{k_{x\mu}=0,1\}} \int \prod_x d\sigma_x \, e^{\beta \sum_{x\mu} k_{x\mu} \left[\sigma_x \cdot \sigma_{x+\mu} - (1-\varkappa/\beta)\right]} \quad . \tag{4.1}$$

In the action the cosine of the angle between neighboring spins is compared with $1-\varkappa/\beta$. This is precisely the expected weak coupling behavior ($\beta \to \infty$) of neighbor correlations for spins in one cluster. Although typical spin fluctuations become smaller when β grows, the combination in the action will keep fluctuating in sign, and the bonds will get strongly correlated to these fluctuations. Spins that are members of different clusters will point in random relative directions on S_{n-1}. A sizable probability to establish an active bond between them is only given if one is inside a cone around the other with an angle of order $\sqrt{\varkappa/\beta}$. It is related to the ratio in area of the intersected part of the sphere to the full sphere and thus proportional to $(\varkappa/\beta)^{\frac{n-1}{2}}$.

To emphasize the rôle played by clusters we may write

$$Z = \sum_{\{k_{x\mu}\}} e^{-\varkappa \sum_{x\mu} k_{x\mu}} \prod_c z_c(k_{x\mu}) \quad . \tag{4.2}$$

The spins in each cluster contribute a complicated weight factor given by the multiple integral

$$z_c = \int \prod_{x \in c} e^{\beta \sum_{c \ni x\mu} k_{x\mu} (\sigma_x \cdot \sigma_{x+\mu} - 1)} \quad . \tag{4.3}$$

For the sum in the exponent no ambiguity arises, since when x and $x+\mu$ are not in the same cluster $k_{x\mu}$ necessarily vanishes. The very definition of clusters guaranties that for $\beta \to \infty$ all spins in c become aligned, and z_c may then be evaluated in perturbation theory (spinwave approximation). Such a calculation is deferred to the appendix, and the result is

$$z_c \simeq \left(|c|\,\beta/2\pi\right)^{\frac{n-1}{2}} C_n \left(\det' K_c\right)^{-\frac{n-1}{2}} \quad . \tag{4.4}$$

Here $|c|$ is the number of spins in c, C_n is the surface of the unit sphere in n dimensions, and the operator under determinant is the diluted lattice Laplacian (A.13). The zero mode has to be omitted in the evaluation of det'. The weak coupling form (4.4) generalizes the factor q for each cluster in the FK-representation of the Potts model. Obviously continuous field variables probe considerably more geometrical details of clusters and incorporate them in the form of complicated weights, when the system is regarded as a correlated percolation process. The features of the O(n) σ-model that enter into the weak coupling evaluation of z_c look consistent with universality: the number of field components and the symmetry structure.

The adaption of the microcanonical Monte Carlo algorithm to O(3)-spins is straightforward for the local

spin and bond updates for which we implemented the heat-bath form. As collective moves we perform rotations of the clusters with elements chosen randomly from O(3) according to the invariant group measure. We found that restrictions to SO(3) or a bias toward the unit element only enhance autocorrelations. For the O(3)σ-model the extra operations of $k_{x\mu}$-updating and cluster analysis and rotation take about 50% of the computer time needed for the spin heatbath, and grows exactly proportional to L^2. These computer times refer to a scalar machine (PDP 10).

In asymptotically free theories the critical point can be approached only from one side at asymptotically vanishing coupling. A simulation at criticality as in the Ising model is hence not possible. In quantum field theory, however, this is not desired anyway as we want physical correlation lengths to stay away from the volume cutoff. To test the diluted form of the σ-model we decided to always choose parameters such that the susceptibility is roughly 10% of the volume for various lattice sizes ($C \cong 0.1$). From data on the standard formulation[21] we estimate that this corresponds to $L/\xi = 3 \ldots 4$ where ξ is the spin correlation length. We think that this is a setting representative for numerical calculations.

We present our data in a form similar to the last section in tables 2...5 for lattices with L=20,28,40,56. The various runs are now distinguished by their bond fraction $\overline{p}_b$ as used in the σ-model version of (3.8) and by β. The chemical potential α and the quantities in the remaining columns are measured. Glancing at the tables we note that the gains we achieve are not as dramatic as in the critical Ising model. Although a quantitative statement is not possible on the basis of our data, we see that the dynamical exponent characterizing the growth of τ with L (and ξ) is probably not vastly different for the diluted and the standard version, and critical slowing down has certainly not been eliminated. On the other hand on the

56^2 lattice we do realize ratios of necessary sweeps for fixed accuracy up to a factor 8 in favor of the new algorithm.

In fig.1a and 1b we show histograms of cluster size distributions on the 40^2 lattice for $\overline{p}_b = .55$ and $\overline{p}_b = .525$. As a reference we also display the analogous distributions for uncorrelated percolation ($\beta = 0$) at $p_b = .51$ and $p_b = .49$, i.e. just above and below the percolation threshold. The similarity in the plots is clearly visible. The peak at large sizes is a precursor of the infinite cluster in an infinite system beyond threshold. We found experimentally that working far below this transition area no criticality is reached with reasonable β-values, while far above it only few large clusters form and the advantage of dynamical dilution fades quickly. From fig.1 we may suspect that in the presence of O(3) spins correlating the bonds the transition moves to $p_b > \frac{1}{2}$ for our β-values. This looks consistent with the perturbative result (4.4) which favors a larger number of smaller clusters as β grows. To conclude this section we would like to remark that the total magnetization that is used as a diagnostic observable for slowing down in refs.[6] and [7] is not useful for our case. When all clusters are rotated with the invariant group measure the spin orientation of the whole system is trivially decorrelated after one sweep.

5. Conclusions

In this article we demonstrated that the Monte Carlo algorithm by Swendsen and Wang for the Ising model is improved further by employing a microcanonical version of it. Our main interest however centered around defining and testing an extension of their method that may be used for theories with continuous dynamical variables. In the two dimensional O(3) σ-model we found that our new formulation, although clearly superior to a standard local heatbath simulation, falls short of offering advantages comparable to those realized in the critical Ising model. A more detailed investigation focusing on long range correlations could shed further light on the profitableness of the new algorithm.

Apart from numerical applications we feel that our concept of adding dynamical dilution to an arbitrary lattice model and analyzing it from a percolation point of view is also of theoretical interest. A key question is if the model really stays in the same universality class as we assumed for the σ-model. We find this hard to decide in the two dimensional model due to the shortage of universal physical quantities. For the application to abelian or nonabelian gauge theory a more complicated labelling algorithm for plaquette percolation clusters has to be developed along the lines of [11]. Otherwise this important extension seems straightforward. For the special case of Z(2) gauge theory an exact equivalence à la FK arises. We hope to return to these issues in the near future.

Acknowledgements

The author would like to thank Burkhard Bunk for supplying him with a subroutine package for estimating autocorrelations and errors. The hospitality of the DESY theory group is gratefully acknowleged.

Appendix

In this appendix we want to compute the weight factor corresponding to one cluster c of O(n)-spins

$$Z_c = \int \prod_{x \in c} d\sigma_x \, e^{\beta \sum_{c \ni x\mu} k_{x\mu} (\sigma_x \cdot \sigma_{x+\mu} - 1)} \tag{A.1}$$

in leading order perturbation theory. In this limit all spins in c are forced to carry out small oscillations around one common direction because by definition of a cluster each pair of spins may be connected by a chain of bonds. Since all overall directions on the sphere are equivalent we have to fix n-1 collective symmetry coordinates before the perturbative expansion of (A.1) can be set up. This is done in the usual way by introducing

$$1 = \Delta(\sigma) \int_{SO(n)} dg \; f(\sigma^g) \Big/ \int dg \tag{A.2}$$

into (A.1). In (A.2) we integrate with the Haar measure over all $g \in SO(n)$, f is a still arbitrary function, and $\Delta(\sigma)$ is defined by (A.2). After changing variables $\sigma \to \sigma^{g^{-1}}$ the group integrations factor out and cancel, and we have

$$Z_c = \int \prod_{x \in c} d\sigma_x \, \Delta(\sigma) f(\sigma) e^{\beta \sum_{c \ni x\mu} k_{x\mu} (\sigma_x \cdot \sigma_{x+\mu} - 1)} \tag{A.3}$$

We define the total spin as

$$S = \sum_{x \in c} \sigma_x \tag{A.4}$$

and choose

$$f(\sigma) = \delta(S^1)\,\delta(S^2)\ldots\delta(S^{n-1})\,\theta(S^n), \qquad (A.5)$$

i.e. the total spin is constrained to lie along the n-axis in spin space. To this choice of f there belongs a compensating Δ,

$$\Delta(\sigma)^{-1} = \frac{1}{|S|^{n-1}} \int dg\, \delta\big((\hat{S}^g)^1\big)\ldots\delta\big((\hat{S}^g)^{n-1}\big)\,\theta\big((\hat{S}^g)^n\big) \Big/ \int dg\,, \qquad (A.6)$$

where $\hat{S}$ is the unit vector in $\mathbb{R}^n$ parallel to S. When g runs over SO(n) the vector $\hat{S}^g$ moves over the sphere S_{n-1}, and in fact the integral in (A.6) is the unique normalized invariant integral over the sphere that we may also write as

$$\Delta(\sigma)^{-1} = \frac{1}{C_n |S|^{n-1}} \int d^nX\, \delta(|X|-1)\,\delta(X^1)\ldots\delta(X^{n-1})\,\theta(X^n) \qquad (A.7)$$

with

$$C_n = \int d^nX\, \delta(|X|-1) = 2\pi^{n/2}/\Gamma(n/2) \qquad (A.9)$$

the surface of the unit sphere in n dimensions. The trivial integration in (A.7) then leaves us with

$$\Delta(\sigma) = |S|^{n-1} C_n\,. \qquad (A.9)$$

Clearly this geometric factor corresponds to the phase space of the rotated copies of c that we exorcized by the fixing function f.

We are now ready for the expansion of (A.3) and parameterize

$$\sigma_x = \big(\varphi_x^1, \varphi_x^2, \ldots, \varphi_x^{n-1}, \sqrt{1-\textstyle\sum(\varphi_x^i)^2}\big) = \big(\vec{\varphi}_x, \sqrt{1-\vec{\varphi}_x^{\,2}}\big). \qquad (A.10)$$

To leading order in $1/\beta$ we have

$$Z_c \simeq C_n |c|^{n-1} \Big\{ \int_{x\in c} \prod d\varphi_x\, \delta\big(\textstyle\sum \varphi_x\big)\, e^{-\frac{\beta}{2}\sum_{c\ni x\mu} k_{x\mu}(\varphi_x-\varphi_{x+\mu})^2} \Big\}^{n-1}. \qquad (A.11)$$

In (A.11) we used $|S| = |c|\,(1+o(1/\beta))$ with $|c|$ the number of spins in c. We dropped all subleading terms in the action as well as in the measure. Also factorization into n-1 identical contributions has been used, and φ_x is a one component field now. The integral may finally be evaluated by introducing an orthonormal system of functions on c that contains the constant $\eta_0(x) = 1/\sqrt{|c|}$. The δ-function takes care of the integration over this mode while the $|c|-1$ remaining ones are gaussian. The result reads

$$Z_c = C_n |c|^{n-1} \Big\{ |c|^{-1/2} (2\pi/\beta)^{\frac{|c|-1}{2}} (\det{}' K_c)^{-1/2} \Big\}^{n-1}. \qquad (A.12)$$

The quadratic form K_c ($|c| \times |c|$ matrix) is read off from the exponent in (A.11)

$$K_c(x,y) = \sum_\mu \big\{ k_{x\mu}(\delta_{x,y} - \delta_{x+\mu,y}) + k_{y\mu}(\delta_{x,y} - \delta_{x,y+\mu}) \big\}. \qquad (A.13)$$

It is a diluted version of the standard lattice Laplacian. Finally we note that factors of the form $A^{|c|}$ in Z_c only affect the normalization of the full partition function Z in (4.2), on which correlations do not depend. Using this freedom to multiply (A.12) by $(\beta/2\pi)^{|c|\frac{n-1}{2}}$ we have derived (4.4).

Footnotes

#1: Note our sign convention for actions; they correspond to negative energy in classical statistical mechanics.

#2: Here we assume implicitly (and correctly for our applications) that Z_m peaks at an $\overline{N}_b < \overline{\overline{N}}_b$ since otherwise the demon would run away[15] with a macroscopic number of bonds. In that case k_D should enter (3.4) with the opposite sign.

#3: Uncorrelated percolation is given by (3.7) with $\beta=0$ and a bond probability $p_b=(1+e^{-\varkappa})^{-1}$.

Table Captions

Table 1: Results of simulations in the two dimensional Ising model.

Table 2: Results of simulations in the O(3) σ-model on a 20^2 lattice.

Table 3: Results of simulations in the O(3) σ-model on a 28^2 lattice.

Table 4: Results of simulations in the O(3) σ-model on a 40^2 lattice.

Table 5: Results of simulations in the O(3) σ-model on a 56^2 lattice.

Figure Captions

Fig.1a: Distribution of cluster sizes in the σ-model run on the 40^2 lattice for $\overline{p}_b=.55$ (see table 4)

Fig.1b: Same as fig.1a for $\overline{p}_b=.525$

Fig.1c: Distribution of cluster sizes for uncorrelated percolation on a periodic 40^2 lattice at $p_b=.51$

Fig.1d: Same as fig.1c for $p_b=.49$

References

[1] M. Lüscher, Phys. Lett. 118B(1982)391.
M. Lüscher, in Progress in Gauge Theories, eds. G. 't Hooft et al. (Plenum, NY 1984).
[2] K. G. Wilson, J. Kogut, Phys. Rep. C12(1974)75.
[3] Monte Carlo Methods in Statistical Physics, ed. K. Binder (Springer, Berlin,1979).
[4] K. Kawasaki, in Phase Transitions and Critical Phenomena, Vol. 2, eds. C. Domb and M. S. Green, (Academic, NY 1972).
J. C. Niel, J. Zinn-Justin, Nucl. Phys. B280[FS17] (1987)355.
[5] G. G. Batrouni, G. R. Katz, A. S. Kronfeld, G. P. Lepage, B. Svetitsky, K. G. Wilson, Phys. Rev. D32(1985)2736.
[6] J. B. Kogut, Nucl. Phys. B275[FS17](1986)1.
[7] J. Goodman, A. D. Sokal, Phys. Rev. Lett. 56(1986)1015.
[8] R. H. Swendsen, J.-S. Wang, Phys. Rev. Lett. 58(1987)86.
[9] P. W. Kasteleyn, C. M. Fortuin, J. Phys. Soc. Jpn. Suppls. 26s(1969)11.
C. M. Fortuin, P. W. Kasteleyn, Physica (Utrecht) 57(1972)536.
[10] U. Wolff, Preprint DESY 87
[11] J. Hoshen, R. Kopelman, Phys. Rev. B14(1976)3438.
[12] M. E. Fisher, Physics 3(1967)255.
[13] K. Symanzik in Mathematical Problems in Theoretical Physics, eds. R. Schrader et al. (Lecture notes in Physics, Springer, Berlin 1982).
[14] N. H. Christ, R. Friedberg, T. D. Lee, Nucl. Phys. B210[FS6](1982)310,337.
[15] M. Creutz, Phys. Rev. Lett. 50(1983)1411.
[16] D. Stauffer, Phys. Rep. 54(1974)1.
J. W. Essam, Rep. Prog. Phys. 43(1980)833.
Percolation Structures and Processes, eds. G. Deutscher, R. Zallen, J. Adler (Hilger, Bristol, 1983).
[17] M. F. Sykes, J. W. Essam, J. Math. Phys. 5(1964)1117.
[18] A. Coniglio, W. Klein. J. Phys. A13(1980)2775.
[19] M. Sweeny, Phys. Rev. B27(1983)4445.
[20] A. Beretti, A. D. Sokal, J. Stat. Phys. 40(1985)483.
[21] Some refs. that we used are:
M. Fukugita, Y, Oyanagi, Phys. Lett. 123B(1983)71.
B. Berg, S. Meyer, I. Montvay, Nucl. Phys. B235[FS11](1984)149.
I. Bender, B. Berg, W. Wetzel, Nucl. Phys. B269(1986)389.

L	type	N_C	E	τ_E	A_E	C	τ_C	A_C	#sw/1000
20	1	-	.7210(10)	40(4)	.21	.5112(43)	46(3)	2.1	200
20	2	17.8	.7225(7)	3.4(1)	.013	.5156(20)	3.4(1)	.11	50
20	3	17.5	.7222(2)	1.4(1)	.00093	.5215(9)	1.5(1)	.019	50
40	1	-	.7138(11)	(140)	.27	.4293(86)	260(40)	9.5	200
40	2	70.7	.7144(5)	4.2(1)	.0051	.4317(19)	4.1(2)	.094	50
40	3	71.0	.7123(1)	1.9(2)	.00034	.4305(9)	2.0(1)	.022	50
80	1	-	.71114(104)	(550)	.22	.3651(135)	750(200)	16	200
80	2	284	.71082(28)	5.3(1)	.0020	.3642(18)	5.5(2)	.091	50
80	3	286	.70884(6)	2.5(3)	.00012	.3576(9)	2.2(1)	.019	50

Table 1

$\overline{Pb}$	β	$\varkappa$	N_C	E	τ_E	A_E	C	τ_C	A_C	#sw/1000
1.	1.3	-	-	.51970(32)	7(2)	.0041	.0952(19)	17(2)	.060	30
.55	4.5	1.95	12.4	.53285(29)	7(1)	.0019	.1004(21)	16(1)	.049	20
.525	5.5	2.01	17.1	.53232(24)	5.0(5)	.0011	.1049(15)	9.0(5)	.025	20
.512	6.5	2.07	20.2	.53572(22)	5.5(8)	.0011	.1105(14)	7.4(3)	.011	20
.5	7.	2.09	22.9	.52605(19)	3.8(1)	.00068	.0997(11)	7.6(3)	.017	20
.475	10.	2.25	29.9	.51804(18)	4.6(5)	.00066	.1031(12)	14(2)	.026	20
.45	17.	2.51	36.7	.50069(17)	5.5(5)	.00064	.1054(14)	21(3)	.044	20

Table 2

$\overline{Pb}$	β	α	N_C	E	τ_E	A_E	C	τ_C	A_C	#sw/1000
1.	1.4	-	-	.56299(23)			.0936(27)	38(2)	.12	30
.55	6.	2.08	27.9	.57329(19)	6(1)	.00071	.1035(22)	19(1)	.052	20
.525	7.5	2.15	38.1	.56335(15)	6(2)	.00058	.0936(15)	18(3)	.038	20
.512	9.	2.23	44.7	.55982(15)	7(3)	.00060	.0999(14)	14(4)	.027	20
.5	11.	2.31	51.6	.55375(15)	6(1)	.00047	.1042(16)	18(4)	.032	20

Table 3

$\overline{Pb}$	β	α	N_C	E	τ_E	A_E	C	τ_C	A_C	#sw/1000
1.	1.5	-	-	.60246(15)	(14)	.0011	.1022(34)	74(7)	.23	50
.55	8.	2.19	66	.60148(11)	8(2)	.00048	.1021(22)	35(5)	.086	30
.525	11.5	2.34	92	.58742(7)	8(2)	.00034	.1071(12)	30(3)	.055	50
.512	12.	2.35	101	.57194(7)	8(3)	.00031	.0892(10)	36(8)	.047	50
.5	15.	2.45	115	.56112(8)	(10)	.00035	.0942(16)	63(7)	.075	30

Table 4

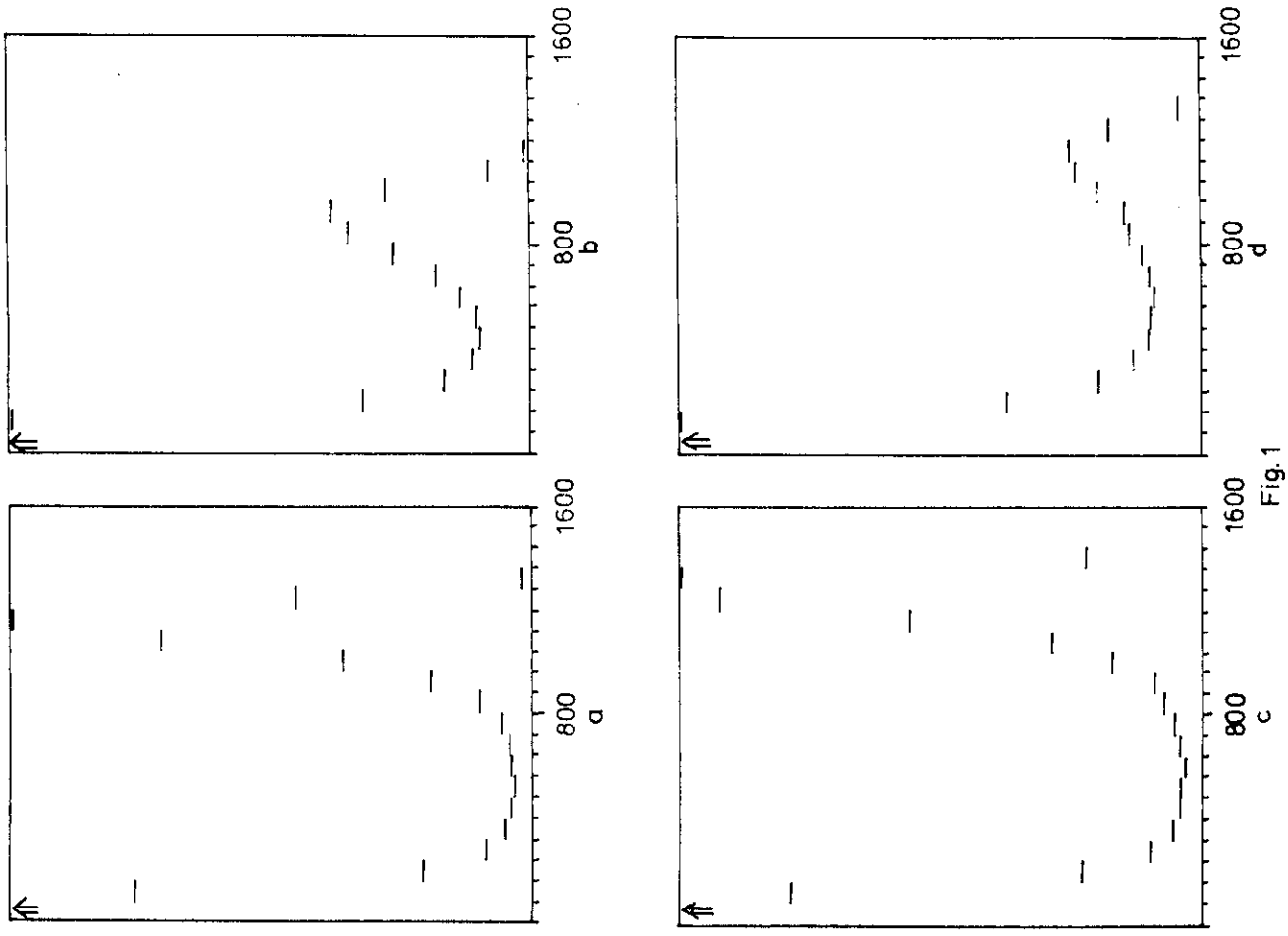

Fig.1

$\bar{P}_b$	ß	$\varkappa$	N_c	E	τ_E	A_E	C	τ_C	A_C	#sw/1000
1.	1.6	-	-	.63612(15)	(21)	.0011	.1094(66)	217(12)	.69	30
.525	15.5	2.46	205	.59326(8)	7(1)	.00013	.1231(23)	75(8)	.083	20
.512	18.	2.52	231	.57687(9)	11(2)	.00020	.1217(26)	108(12)	.088	20

Table 5